

From Drought to Dinner: Climate Shocks and Food Import Inflation

Chulwon Park*
*Department of Economics
Sogang University*

(Dated: December 8, 2025)

How do climate shocks in major agricultural exporting regions transmit into food-importing economies? This paper uses satellite-derived drought indices as proxies for physical supply constraints in the United States, Brazil, Australia, Canada, and Russia, tracing their transmission into Korean grain and oilseed imports and domestic inflation. Using panel local projections that control for global commodity prices, I isolate supply-side disruptions net of information already reflected in markets. A one-standard-deviation increase in drought severity generates import reductions of 13–17 percentage points, with the Vegetation Condition Index producing the fastest response (8 percentage points within two months, peaking at 15 percentage points). These effects remain large and statistically significant after controlling for global prices, confirming orthogonality to market-aggregated information. The transmission extends into domestic food inflation: Korea's grain CPI increases 0.3–0.7 percentage points (unweighted) and 1.0–1.3 percentage points (weighted by import shares). The Evaporative Stress Index exhibits a revealing divergence—no quantity effects but significant price increases—indicating that early-stage water stress operates through market expectations rather than binding physical constraints. These findings demonstrate that real-time satellite monitoring provides actionable early warnings for strategic reserve management and inflation forecasting in structurally import-dependent economies.

I. INTRODUCTION

South Korea's food system is structurally exposed to external climate shocks. With grain self-sufficiency near 20 percent and consumer food prices 45–50 percent above the OECD average, drought events in major exporting regions can rapidly translate into import supply pressures and domestic price volatility. Understanding how climate shocks propagate into Korean markets is essential for both food security policy and inflation forecasting.

The key challenge is that agricultural supply chains operate with substantial temporal lags. Drought conditions during the growing season constrain planting decisions, stunt crop development, and reduce harvestable yields, which subsequently limit export availability and depress import flows months later. Yet official production statistics—the conventional basis for forecasting trade adjustments—appear only after harvest, when supply disruptions have already materialized. This paper addresses this information gap by using satellite-derived drought indices as high-frequency proxies for physical supply constraints in major exporting regions. The predictive power of satellite monitoring stems from its ability to capture biophysical stress during critical growth stages, enabling real-time assessment of emerging supply shocks before they propagate through trade channels.

I develop an empirical framework interpreting satellite indices as proxies for binding supply constraints rather

than market-observable signals. Controlling for global commodity prices, exchange rates, and macroeconomic conditions, I estimate how vegetation stress, soil moisture deficits, and evapotranspiration anomalies translate into Korean import adjustments and domestic inflation. The estimated coefficients isolate supply-side disruptions net of information already reflected in market prices, directly measuring the component of trade variation attributable to biophysical constraints that operate independently of price-mediated market adjustments. This approach differs from conventional analyses that treat climate variables as predictive signals for market participants; instead, I quantify how physical availability constraints—captured by satellite data but not fully priced in contemporaneous markets—generate quantity and price responses along specific country-commodity pathways.

I construct three complementary monthly drought indicators from satellite data: the Vegetation Condition Index (VCI), which normalizes NDVI relative to historical ranges; the Evaporative Stress Index (ESI), which captures early-stage water stress through transpiration anomalies; and the Soil Moisture Index (SMI), which measures root-zone moisture availability. Using monthly Korean import data disaggregated by commodity and origin, combined with satellite indices for the United States, Brazil, Australia, Canada, and Russia, I estimate dynamic responses via panel local projections over twelve- to twenty-four-month horizons.

The analysis yields three main findings. First, vegetation and soil moisture indices capture economically significant physical supply shocks: a one-standard-deviation increase in drought severity generates cumulative import

* inuuniw@u.sogang.ac.kr

reductions of 13–17 percentage points, with peak contractionary effects occurring three to eight months after the shock. ESI exhibits negligible effects on import quantities, suggesting that evapotranspiration anomalies do not constitute binding constraints on export availability once vegetation and soil conditions are accounted for.

Second, VCI emerges as the most powerful and immediate proxy for supply disruptions. Import quantities contract by 8 percentage points within two months of a vegetation-based drought shock and reach peak declines of 15 percentage points by month five. This faster transmission relative to soil moisture shocks reflects the direct linkage between satellite-observed vegetation stress and harvestable biomass: when NDVI indicates severe wilting during critical reproductive stages, the physical constraint on exportable supply materializes rapidly. In contrast, SMI exhibits a delayed buildup, consistent with the biological lag between root-zone moisture deficits at planting and subsequent yield losses. Crucially, these effects remain large and statistically significant even after controlling for contemporaneous global commodity prices, confirming that satellite indices capture supply disruptions orthogonal to price information already aggregated in markets.

Third, the transmission extends beyond import quantities into domestic food inflation. Korea’s grain CPI increases by 0.3–0.7 percentage points in response to unweighted drought shocks, with VCI and SMI generating the largest effects consistent with their role as physical supply constraint proxies. The response to ESI is particularly revealing: while negligible for quantities, it is positive and statistically significant for prices, indicating that early-stage evapotranspiration anomalies operate through market expectation channels rather than binding physical constraints. When drought indices are weighted by each exporter’s share in Korea’s import basket, effects amplify dramatically—weighted VCI and ESI shocks generate domestic grain inflation of 1.0–1.3 percentage points over 12–18 months. This amplification reflects Korea’s concentration risk: the United States and Brazil collectively account for the majority of grain and oilseed imports, and drought conditions in these dominant suppliers generate disproportionate price impacts through both physical availability constraints and market risk premia.

Disaggregation by origin and commodity reveals substantial heterogeneity. Brazilian imports exhibit particularly large drought sensitivity (20–30 percentage point declines), consistent with Brazil’s dominant role in global soybean markets. Russian and Canadian imports show similarly large elasticities, with timing patterns reflecting hemisphere-specific harvest calendars. Across commodities, cereals exhibit the largest responses (20–30 percentage points), reflecting their centrality to food security and limited substitutability, while oilseeds show more

moderate effects (10–20 percentage points).

From a policy perspective, these findings demonstrate that real-time satellite monitoring provides actionable early warnings for strategic reserve management, supplier diversification, and inflation forecasting. For an economy where consumer food prices stand 45–50 percent above the OECD average and grain self-sufficiency hovers near 20 percent, a one-standard-deviation drought shock in major exporting regions implies 10–30 percentage point reductions in import quantities and up to 1.3 percentage points of domestic grain inflation over the subsequent year. The fast transmission of VCI shocks—with significant effects within two to three months—enables near-term reserve decisions and forward contracting.

Crucially, the predictive power of satellite indices remains robust even after controlling for global commodity prices. This orthogonality validates the independent value of satellite monitoring beyond merely tracking market prices: vegetation and soil moisture signals capture physical availability risks—such as logistical bottlenecks, quality degradation, or contract force majeure—that are not fully priced in contemporaneous spot markets. This information advantage is particularly valuable for import-dependent economies with limited supplier diversification options.

The remainder of the paper proceeds as follows. Section II describes the data construction. Section III presents the panel local projection framework. Section IV reports baseline and heterogeneous impulse responses. Section V concludes.

Literature.

This paper connects three literatures. First, substantial research documents climate variability’s impact on agricultural yields, with ENSO studies showing how temperature and precipitation shocks generate output variation across regions[1, 2]. Econometric approaches to measuring climate impacts on agriculture have been refined through panel methods and spatial analysis[3, 4]. However, this work typically relies on annual data and does not trace transmission into trade flows at high frequency.

Second, recent contributions incorporate trade channels. Evidence shows climate disasters raise agricultural imports[5] and governments alter trade policy in response to rainfall shocks[6]. Research on food price transmission demonstrates that international commodity price shocks propagate into domestic markets through trade linkages[7, 8], with implications for food security in import-dependent economies[9]. Yet these studies operate at aggregate levels without modeling granular country-product pathways or exploiting high-frequency climate signals.

A common limitation is reliance on ex-post production data. Because production statistics appear only after harvest, they cannot serve as real-time state variables for forecasting supply disruptions. High-frequency monitoring of evolving crop conditions during the growing season provides a temporal information advantage over conventional production-based approaches. Work on agricultural futures markets shows that weather information during critical growth periods is rapidly incorporated into prices[10, 11], underscoring the importance of real-time climate monitoring for market forecasting.

Satellite remote sensing offers a solution through global, objective, high-frequency measurements. MODIS NDVI products enable VCI construction[12, 13], evapotranspiration products support ESI derivation[14], and ERA5-Land provides soil moisture data[15]. These indices at monthly frequency enable continuous monitoring of agricultural conditions and have been operationalized in famine early warning systems[16, 17]. Recent advances demonstrate satellite data's utility for yield forecasting[18] and drought monitoring[19], though applications to bilateral trade forecasting remain limited.

This paper uses satellite-derived drought indices as proxies for physical supply constraints in a framework tracing their transmission into trade flows and domestic prices along specific country–crop pathways. Rather than treating satellite data as market-observable signals that influence trader behavior, I interpret them as direct measurements of biophysical stress that constrains export availability independently of price adjustments. The panel local projection approach[20, 21] estimates flexible impulse responses without imposing parametric VAR restrictions, allowing data-driven identification of adjustment timing and heterogeneity across commodities and origins. Controlling for global commodity prices throughout the estimation ensures that the identified effects reflect physical supply disruptions orthogonal to information already aggregated in market prices.

II. DATA

The empirical analysis combines monthly trade statistics for Korean food and feed imports, satellite-derived drought indicators for major exporting regions, and macroeconomic control variables.

A. Korean Trade Data

Import data are drawn from the Korea International Trade Association statistics platform at the Harmonized System level. The analysis focuses on five HS 2-digit cat-

egories central to Korean food security: cereals (HS 10), milling products (HS 11), oilseeds (HS 12), fats and oils (HS 15), and residues for livestock feed (HS 23). Monthly import volumes and values are extracted by origin country, covering December 2002 through May 2023. Unit values serve as proxies for border prices. Import quantities are measured in physical units (metric tons), while import values are expressed in U.S. dollars and converted into real terms using the GDP deflator with base year [2015 = 100]. Unit values (dollars per kg) are deflated using the same price index so that all value-based variables used in the regressions are in constant prices before taking logarithms.

Five major supplier countries are retained: the United States, Australia, Brazil, Canada, and Russia. These countries collectively account for a substantial share of Korean grain and oilseed imports and exhibit sufficient regional production concentration to permit meaningful linkage with satellite-derived indicators. Argentina and Ukraine are excluded due to incomplete availability of monthly uncertainty indices over the study period.

B. Satellite-Derived Drought Indices

High-frequency drought indicators are constructed through raw data acquisition from Google Earth Engine, normalization relative to region- and month-specific climatologies, and aggregation to monthly regional averages. Five agriculturally important regions are analyzed: the U.S. Corn Belt, Brazil's Mato Grosso, Canada's Prairies, Australia's Wheat Belt and Southern Russia.[22]

The Vegetation Condition Index[12, 13] is defined as

$$VCI_{r,t} = 100 \times \frac{NDVI_{r,t} - NDVI_{r,m}^{\min}}{NDVI_{r,m}^{\max} - NDVI_{r,m}^{\min}}, \quad (1)$$

where r indexes regions, t indexes time, and m denotes calendar month. VCI expresses current vegetation as a percentile of the historical range, removing seasonal cycles. High values indicate favorable conditions; low values signal stress.

The Evaporative Stress Index[14] standardizes evapotranspiration anomalies:

$$ESI_{r,t} = \frac{ET_{r,t} - \mu_{r,m}}{\sigma_{r,m}}, \quad (2)$$

where $\mu_{r,m}$ and $\sigma_{r,m}$ are the mean and standard deviation of evapotranspiration for region r and month m . Negative ESI values indicate water stress when stomatal closure reduces transpiration before visible wilting occurs.

The Soil Moisture Index follows VCI normalization:

$$\text{SMI}_{r,t} = \frac{\text{SM}_{r,t} - \text{SM}_{r,m}^{\min}}{\text{SM}_{r,m}^{\max} - \text{SM}_{r,m}^{\min}}, \quad (3)$$

where minimum and maximum values are computed over all observations in calendar month m . Low SMI values indicate dry soil that constrains planting decisions and early growth.

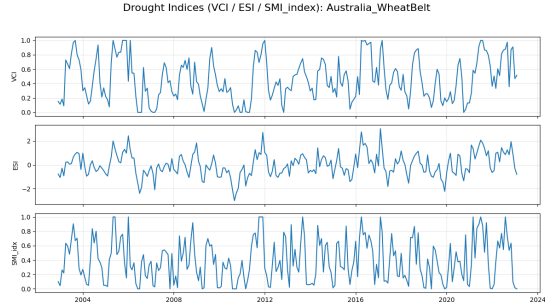


FIG. 1: Drought Indices for Australia’s Wheat Belt

a

^a Note: Indices are normalized relative to month-specific historical distributions to remove seasonal patterns. VCI and SMI range from 0 (drought) to 100 or 1 (favorable conditions); ESI is expressed as a standardized z-score.

All drought indices used in the empirical analysis are aggregated to monthly region-level values using a consistent two-step procedure implemented in Google Earth Engine (GEE). First, all satellite scenes occurring within a given month are averaged to construct a monthly composite for each underlying physical variable (e.g., NDVI, evapotranspiration, soil moisture). Formally, for each pixel r in region R and month t ,

$$X_{r,t} = \frac{1}{N_t} \sum_{k \in t} X_{r,k},$$

where N_t is the number of observations available in month t . Second, each regional monthly value is obtained as the spatial mean of the monthly composite over the region’s bounding box:

$$\bar{X}_{R,t} = \frac{1}{|R|} \int_{r \in R} X_{r,t} dr.$$

In practice, the spatial integral is computed via *reduceRegion(mean)* in GEE, which averages all valid pixels within the region at their native resolution (1 km for NDVI, 500 m for ET, and 0.1° for ERA5 soil moisture).

These spatially averaged monthly series $\bar{X}_{R,t}$ form the basis for constructing region-level drought indices. For the Vegetation Condition Index (VCI), the monthly NDVI composite is first averaged over the region, then normalized relative to the region- and month-specific historical minimum and maximum:

$$\text{VCI}_{R,t} = 100 \times \frac{\bar{\text{NDVI}}_{R,t} - \min_{s \in m(t)} \bar{\text{NDVI}}_{R,s}}{\max_{s \in m(t)} \bar{\text{NDVI}}_{R,s} - \min_{s \in m(t)} \bar{\text{NDVI}}_{R,s}}.$$

Thus, VCI measures how current vegetation compares with its historical range for that month, abstracting from seasonality. The Evaporative Stress Index (ESI) is computed by standardizing the region-level evapotranspiration anomaly within each calendar month:

$$\text{ESI}_{R,t} = \frac{\bar{\text{ET}}_{R,t} - \mu_{R,m(t)}}{\sigma_{R,m(t)}},$$

where $\mu_{R,m}$ and $\sigma_{R,m}$ are the mean and standard deviation of $\bar{\text{ET}}_{R,t}$ across all years for calendar month m .

Finally, the Soil Moisture Index (SMI) applies the same min–max normalization as VCI to the region-level ERA5 surface soil moisture series:

$$\text{SMI}_{R,t} = \frac{\bar{\text{SM}}_{R,t} - \min_{s \in m(t)} \bar{\text{SM}}_{R,s}}{\max_{s \in m(t)} \bar{\text{SM}}_{R,s} - \min_{s \in m(t)} \bar{\text{SM}}_{R,s}}.$$

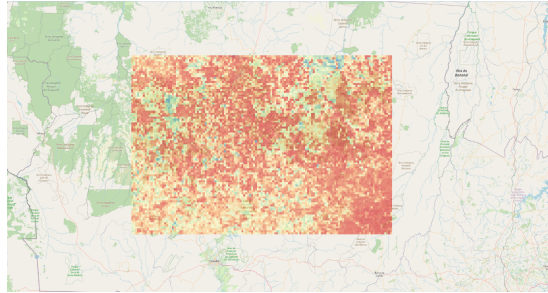
This approach ensures that all indices reflect anomalies relative to each region’s own climatological distribution, thereby removing seasonal cycles and making conditions comparable across time. Prior to estimation, all three indices are standardized to have mean zero and unit variance within each region, so that regression coefficients are interpretable per one-standard-deviation change in the index.

To facilitate economic interpretation in the empirical analysis, the standardized indices are sign-inverted prior to estimation. In the raw construction (Equations 1–3), higher values denote favorable moisture or vegetation conditions (i.e., less drought). However, to ensure that the estimated impulse response functions intuitively reflect reactions to “drought shocks,” the standardized variables are multiplied by -1 . Consequently, in all subsequent regression results and figures, a positive shock ($+1\sigma$) represents an increase in drought severity (a deterioration in crop conditions). This linear transformation aligns the visual representation with the concept of a drought event without altering the statistical properties or validity of the underlying data.

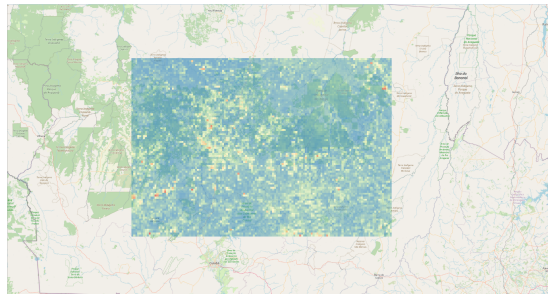
C. Macroeconomic and Trade Control Variables

To isolate the marginal predictive content of drought indicators, specifications control for macroeconomic and trade-related variables influencing Korean imports. Inclusion of these controls ensures that the estimated drought coefficients capture physical supply shocks rather than responses to broader global market fluctuations.

First, to capture global market price signals, I utilize monthly nominal commodity prices from the World Bank Commodity Price Data (The Pink Sheet). Specific

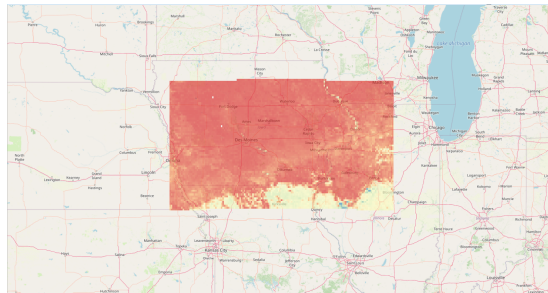


(a) Brazil (Mato Grosso), VCI, 2016/07: Severe drought episode.

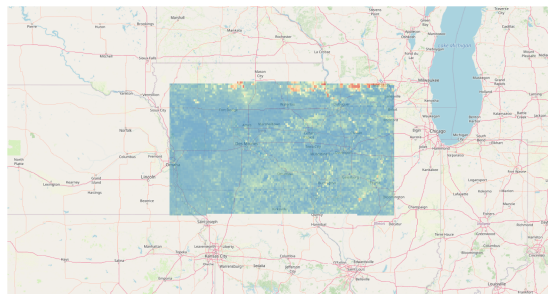


(b) Brazil (Mato Grosso), VCI, 2015/01: Favorable vegetation conditions.

FIG. 2: Vegetation stress in Brazil’s Mato Grosso: comparison between a peak drought month and a favorable growing period, based on VCI derived from MODIS NDVI.



(a) U.S. Corn Belt (Iowa-centered), VCI, 2010/02: Severe winter drought.



(b) U.S. Corn Belt (Iowa-centered), VCI, 2017/02: Above-normal vegetation conditions.

FIG. 3: Vegetation conditions in the U.S. Corn Belt: contrasting a drought-affected month with a period of favorable moisture conditions, using VCI constructed from MODIS NDVI.

benchmarks include Maize, Wheat (US Soft Red Winter), Soybeans, and Barley. Controlling for these global price benchmarks is essential to distinguish whether import adjustments are driven by satellite-detected physical constraints or simply by importers reacting to observable price movements.

Second, shipping and energy costs are critical for a trade-dependent economy like Korea. Monthly crude oil prices (WTI spot) are included since energy represents a significant component of both agricultural production costs (fertilizer, fuel) and international freight rates. The Baltic Dry Index (BDI) is added to explicitly control for variations in bulk shipping costs, which can drive a wedge between border prices and exporter farm-gate prices.

Third, bilateral exchange rates are included to account for changes in Korea’s relative purchasing power, which directly affects import demand elasticity. GDP growth rates for each exporter are also controlled to capture domestic demand shocks within exporting countries that might crowd out exports independent of climate conditions.

Fourth, I control for domestic demand-pull inflationary pressures in Korea to ensure that the estimated coefficients reflect external supply shocks rather than local business cycle fluctuations. Since GDP data is only available quarterly, I utilize the Industrial Production Index (IPI) and the unemployment rate from the Korean Statistical Information Service (KOSIS) as monthly proxies for real economic activity and labor market tightness, respectively. Additionally, the 3-year Treasury Bond Yield, obtained from the Bank of Korea’s Economic Statistics System (ECOS), is included to control for the market interest rate environment and domestic liquidity conditions. Inclusion of these high-frequency domestic indicators is essential to mitigate omitted variable bias arising from Korea’s internal economic dynamics.

Finally, three indices capturing global uncertainty and risk enter in logarithmic form. The Economic Policy Uncertainty index[23] measures policy-related uncertainty, while the Geopolitical Risk index[24] quantifies international tensions. The VIX serves as a proxy for financial market stress[25]. These variables are crucial for controlling for “precautionary” behavior; for instance, importers might engage in panic buying or delay contracts during periods of high global volatility, irrespective of agricultural growing conditions.

For the domestic price transmission analysis (Section 4.2), the dependent variable is the grain component of Korea’s Consumer Price Index (CPI), obtained from the Bank of Korea’s Economic Statistics System (ECOS). The grain CPI is a monthly index capturing retail prices of cereals and grain-based products consumed domestically, providing a direct measure of how external supply shocks transmit into household food costs. The index is

seasonally adjusted and expressed in logarithmic form to facilitate interpretation of percentage changes in response to drought shocks.

III. EMPIRICAL FRAMEWORK

A. Baseline Framework

The empirical strategy employs panel local projections to estimate the dynamic response of Korean import volumes to standardized drought shocks in exporting regions. Local projections[20] offer a flexible nonparametric alternative to vector autoregressions, particularly well suited to panel settings with fixed effects and clustered standard errors.

For each country–crop pathway indexed by i and month t , the cumulative response of imports at horizon h is estimated via the regression

$$y_{i,t+h} - y_{i,t} = \alpha_{i,h} + \delta_{m,h} + \beta_h z_{i,t} + \mathbf{x}'_{i,t} \boldsymbol{\gamma}_h + \varepsilon_{i,t,h}, \quad (4)$$

where $y_{i,t}$ denotes the log of import value or quantity, $z_{i,t}$ is a standardized drought index (VCI, ESI, or SMI) for the exporting region associated with pathway i at time t . The control vector $\mathbf{x}_{i,t}$ includes the logarithm of the relevant global commodity price (e.g., global wheat price for wheat imports) to ensure that β_h captures weather information not yet priced in global markets. Additionally, $\mathbf{x}_{i,t}$ includes the bilateral exchange rate, crude oil prices, shipping costs, and the logarithms of economic policy uncertainty, geopolitical risk, and the VIX. The terms $\alpha_{i,h}$ and $\delta_{m,h}$ represent pathway and calendar-month fixed effects, both allowed to vary freely across horizons. Standard errors are two-way clustered by pathway and month to account for arbitrary serial correlation within pathways and common shocks across pathways in the same month.

The coefficient β_h measures the cumulative change in log imports h months after a one-standard-deviation increase in drought severity. Interpreting $z_{i,t}$ as a proxy for physical supply constraints, a negative β_h would indicate that biophysical stress in exporting regions translates into reduced export availability and subsequent import contractions. The inclusion of global prices in $\mathbf{x}_{i,t}$ ensures that β_h captures the quantity adjustment driven by physical supply shocks net of the price information already aggregated in global commodity markets. In other words, the estimated coefficients isolate the component of trade variation attributable to biophysical constraints that operate independently of price-mediated market adjustments.

In the baseline specification, equation (4) is estimated separately for each drought index, so that $z_{i,t}$ denotes

either VCI, ESI, or SMI in turn. To assess whether the results are driven by a single preferred proxy or by a common underlying drought factor, I also estimate a multi-index specification in which $z_{i,t}$ is replaced by the vector $\mathbf{z}_{i,t} = (\text{VCI}_{i,t}, \text{ESI}_{i,t}, \text{SMI}_{i,t})'$ and the coefficient of interest becomes the corresponding horizon-specific vector $\boldsymbol{\beta}_h$. The impulse responses obtained from this joint specification are very similar in magnitude and timing to those from the single-index regressions, suggesting that multicollinearity among the three indices does not materially affect the estimated dynamic responses.

The local projection approach has several advantages. It does not impose strong lag restrictions inherent in VARs, allowing nonmonotonic or asymmetric response profiles. Horizon-by-horizon estimation accommodates time-varying fixed effects, capturing seasonal import patterns and persistent heterogeneity across pathways. The framework easily handles high-dimensional fixed effects without incurring dimensionality problems. Finally, cumulative responses $y_{i,t+h} - y_{i,t}$ ensure direct comparability to traditional moving-average representations of dynamic causal effects.

B. Transmission to Domestic Prices

While the baseline analysis quantifies trade volume adjustments along specific bilateral pathways, a critical policy question is whether these external supply shocks pass through to domestic food inflation. To assess this, I extend the local projection framework to estimate the response of Korea's sectoral Consumer Price Index (CPI) to foreign drought shocks.

I employ a dual-specification strategy to test price transmission. First, I estimate a baseline specification using the unweighted standardized drought indices ($z_{i,t}$). This tests whether climate anomalies in exporting countries, on average, have any discernible impact on Korean inflation regardless of the supplier's market share. Second, to account for the heterogeneity in supplier importance, I estimate a weighted specification where the drought index is interacted with the exporter's share in Korea's import basket.

For the weighted specification, I define a time-invariant import weight w_i for each country i as its share of total sectoral imports over the sample period:

$$w_i = \frac{\sum_t M_{i,t}}{\sum_j \sum_t M_{j,t}}, \quad (5)$$

where $M_{i,t}$ represents the real import value from origin i . The weighted shock is then defined as $z_{i,t} \times w_i$. This ensures that a shock in a dominant supplier (e.g., U.S. maize) is scaled up, while a shock in a marginal supplier is down-weighted.

Since the dependent variable (Korean CPI) is an aggregate time-series common to all pathways, including time fixed effects would absorb all variation in the outcome. Instead, I control for linear and quadratic time trends (t, t^2) to account for secular inflation dynamics. The estimation equations for the unweighted (Baseline) and weighted (Interaction) models are, respectively:

$$\Delta_h y_{i,t+h} = \alpha_{i,h} + \beta_h S_{i,t} + \mathbf{X}'_t \gamma_h + \lambda_h^1 t + \lambda_h^2 t^2 + \varepsilon_{i,t,h} \quad (6)$$

where $S_{i,t}$ denotes the drought shock variable, defined as:

- $S_{i,t} = z_{i,t}$ in the baseline specification (unweighted).
- $S_{i,t} = z_{i,t} \times w_i$ in the interaction specification (weighted).

The control vector \mathbf{X}_t is expanded to explicitly distinguish external supply shocks from domestic demand-pull inflation. In addition to global cost factors (commodity prices, oil, exchange rates, risk indices), I control for Korea's internal macroeconomic conditions: the unemployment rate (labor market slack), the Industrial Production Index (real economic activity), and the 3-year Treasury Bond Yield (domestic interest rate and liquidity conditions). This specification ensures that the estimated coefficients β_h and β_h^w capture the causal impact of foreign climate shocks on domestic prices, net of global trends and local business cycles.

IV. RESULTS

This section presents the estimated impulse responses of Korean food and feed import quantities to standardized drought shocks in major exporting regions. The analysis interprets satellite-derived drought indices as proxies for physical supply constraints in agricultural production, capturing biophysical stress that operates independently of price-mediated market adjustments. Because the specification controls for global commodity prices, bilateral exchange rates, and macroeconomic conditions, the estimated coefficients β_h isolate the component of import variation attributable to supply-side disruptions net of the information already reflected in market prices. All drought indices are standardized to have mean zero and unit variance and sign-inverted so that a positive shock represents increased drought severity (worsening crop conditions). Estimated coefficients therefore represent the percentage-point change in log imports associated with a one-standard-deviation increase in physical water stress.

Comparison across the three indices reveals a clear hierarchy. VCI generates the largest and fastest response,

consistent with its direct measurement of crop biomass. SMI exhibits delayed but persistent effects, reflecting the temporal lag between root-zone moisture and final harvest outcomes. ESI shows no systematic relationship. These results demonstrate that VCI and SMI provide information orthogonal to market prices, enabling quantification of physical disruptions to Korean food import channels.

The aggregate patterns mask substantial heterogeneity across origin countries and commodities. Country-specific estimates reveal that Korean imports from Brazil exhibit particularly large responses to VCI and SMI shocks (20–30 percentage point declines), consistent with Brazil's dominant role in global soybean markets and the concentration of production in Mato Grosso. Russian and Canadian imports show similarly large elasticities, with timing patterns reflecting hemisphere-specific harvest calendars. Commodity disaggregation further demonstrates that cereals (HS 10) exhibit the largest drought sensitivity (20–30 percentage point responses to VCI and SMI), while oilseeds (HS 12) show more moderate effects (10–20 percentage points), likely reflecting greater storage capacity and industrial flexibility in oilseed supply chains. Detailed country- and commodity-specific impulse responses are reported in Appendix B.

A. Aggregate Import Responses

Figure 4 presents the impulse responses of Korean grain and oilseed imports to standardized drought shocks across the three satellite-derived indices.

Panel (a) reports the response to evapotranspiration-based drought stress (ESI). The response remains near zero and statistically insignificant throughout the horizon, with point estimates never exceeding 2–3 percentage points. This null result suggests that evapotranspiration anomalies do not capture economically relevant supply constraints once vegetation and soil moisture conditions are controlled.

Panel (b) presents the response to soil moisture shocks. Effects emerge after three months, reaching a trough of –16 to –17 percentage points around months five through six before stabilizing near –13 to –15 percentage points. This delayed adjustment reflects the biological transmission mechanism: soil moisture deficits constrain planting and early-stage crop establishment, which propagate into yield losses and reduced export availability. The magnitude is economically substantial—a one-standard-deviation deterioration generates 13–17 percentage point import reductions even after controlling for global commodity prices, indicating that soil moisture shocks capture supply disruptions orthogonal to contemporaneous price signals.

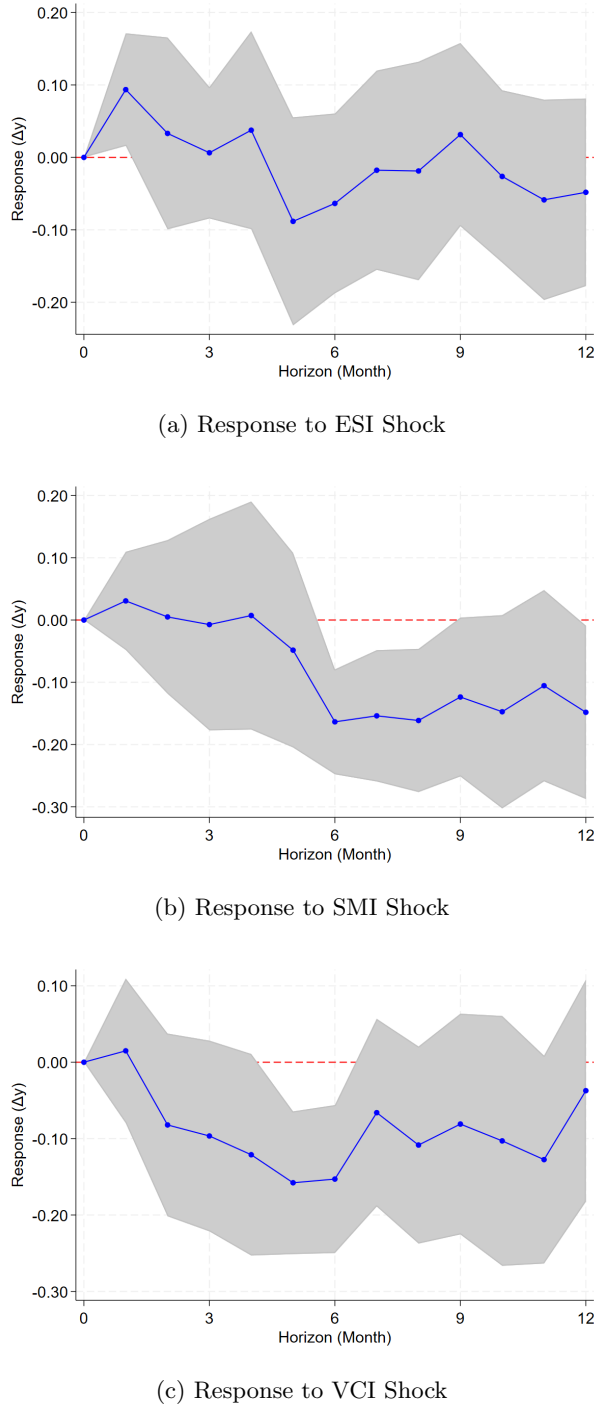


FIG. 4: Impulse Response of Import Quantities to Drought Index Shocks (Baseline)

Panel (c) shows the Vegetation Condition Index response, which exhibits the sharpest contraction. Imports fall 8 percentage points within two months and reach a peak decline of 15 percentage points by month five. The faster transmission reflects the direct linkage between vegetation stress and harvestable biomass: satellite-derived NDVI captures crop conditions during critical reproduc-

tive stages, generating binding constraints on exportable supply more rapidly than soil moisture deficits, which must first propagate through planting and early development.

The magnitude and timing confirm that VCI serves as a powerful proxy for physical supply constraints. Crucially, the effect remains large and significant after controlling for global prices, implying that the physical reduction in export availability operates through channels not fully reflected in contemporaneous price information—consistent with institutional features such as forward contracts, force majeure clauses, and spot market availability constraints.

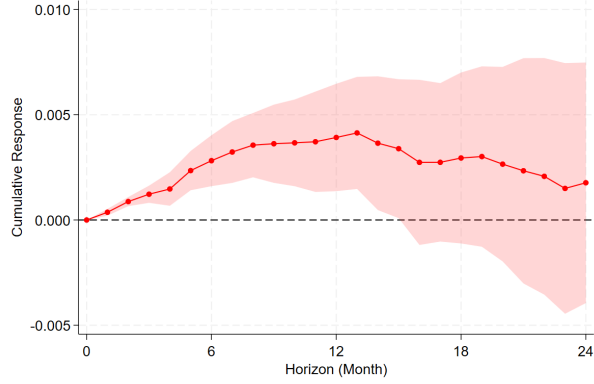
Comparison across the three indices reveals a clear hierarchy. VCI generates the largest and fastest response, consistent with its direct measurement of crop biomass. SMI exhibits delayed but persistent effects, reflecting the temporal lag between root-zone moisture and final harvest outcomes. ESI shows no systematic relationship. These results demonstrate that VCI and SMI capture physical supply shocks that reduce Korean import quantities by 13–17 percentage points within 3–8 months.

A critical policy question is whether these quantity reductions—driven by binding physical constraints in exporting regions—transmit into domestic food inflation, or whether Korean consumers are insulated through substitution, inventory drawdown, or domestic production adjustments. Korea’s structural features—grain self-sufficiency near 20 percent, limited strategic reserves, and high supplier concentration in the United States and Brazil—suggest strong pass-through from quantity shocks to price increases. Section 4.2 examines this transmission mechanism, testing whether the same drought shocks that contract import volumes also generate domestic grain inflation.

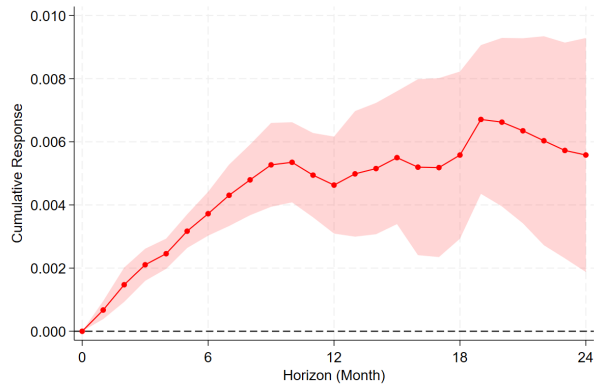
B. Transmission to Domestic Prices

The import quantity reductions documented in Section 4.1 represent the first stage of climate shock transmission: physical constraints in exporting regions reduce Korea’s access to foreign grain supply by 13–17 percentage points. This section examines the second stage: whether reduced import availability translates into higher domestic food prices.

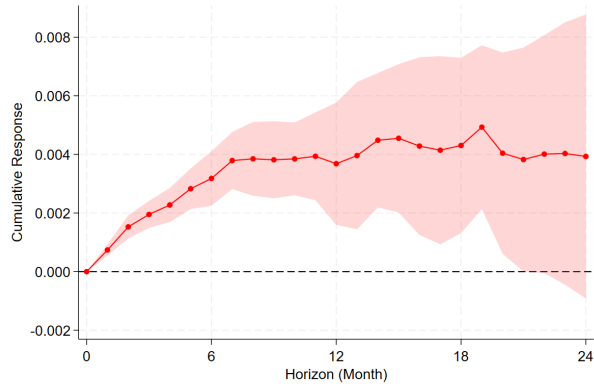
Standard supply-demand analysis predicts that negative supply shocks—holding demand constant—generate price increases. However, the magnitude of transmission depends on several structural factors: the elasticity of domestic demand, the availability of inventory buffers, the speed of domestic production adjustment, and the degree of import concentration in dominant suppliers. Korea’s



(a) Response to ESI Shock



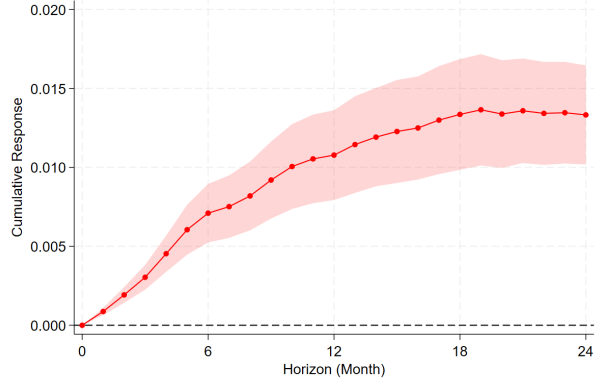
(b) Response to SMI Shock



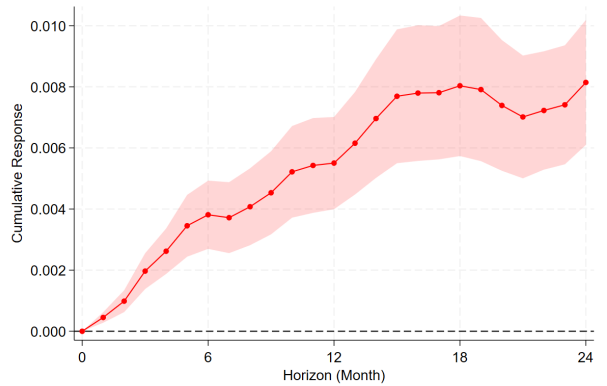
(c) Response to VCI Shock

FIG. 5: Impulse Response of CPI (Grain) to Drought Index Shocks: Unweighted

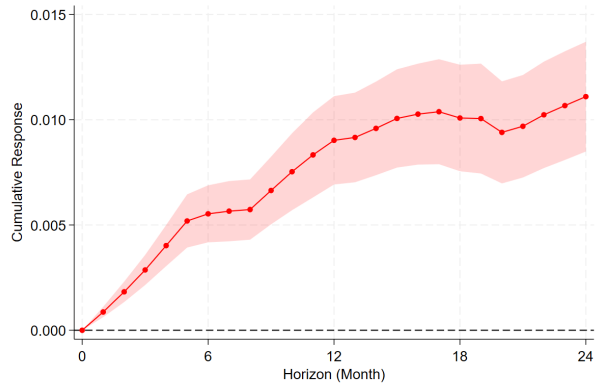
structural characteristics—grain self-sufficiency near 20 percent, limited strategic grain reserves relative to consumption, and high import concentration in the United States and Brazil—suggest strong pass-through from import quantity contractions to domestic inflation. Moreover, the bilateral nature of the supply shocks identified in Section 4.1 implies that Korean importers cannot easily substitute toward alternative origins when droughts concentrate in major suppliers.



(a) Response to ESI Shock (Weighted)



(b) Response to SMI Shock (Weighted)



(c) Response to VCI Shock (Weighted)

FIG. 6: Impulse Response of CPI (Grain) to Drought Index Shocks: Weighted by Import Share

Figures 5 and 6 test this prediction by estimating the response of Korea's grain Consumer Price Index to the same standardized drought shocks that generated import reductions in Section 4.1. The estimation uses both

unweighted drought indices (testing average transmission) and import-share weighted indices (testing whether shocks in dominant suppliers generate disproportionate price effects consistent with market power and limited substitutability).

Figure 5 reports baseline results using unweighted drought indices. Panel (a) shows the response to ESI shocks. Unlike the quantity results where ESI had no effect, CPI exhibits a delayed but persistent increase, reaching 0.3–0.4 percentage points around month 7 and remaining elevated through month 16 before converging to zero. Panel (b) presents the SMI response, which rises gradually to 0.5 percentage points by month 6 and peaks near 0.7 percentage points around month 18. Panel (c) shows the VCI response, which increases rapidly to 0.4 percentage points by month 6 and stabilizes around this level through the remainder of the horizon. All three indices generate positive and statistically significant price effects, confirming that the physical supply constraints documented in Section 4.1 transmit into domestic inflation.

Figure 6 presents results using import-share weighted indices, which scale each country’s drought shock by its importance in Korea’s grain import basket. The weighted specification reveals dramatic amplification across all indices. Panel (a) shows that weighted ESI effects reach 1.3 percentage points by month 18—roughly 3–4 times larger than the unweighted estimate. Panel (b) demonstrates that weighted SMI effects peak near 0.8 percentage points, modestly larger than the unweighted case. Panel (c) shows that weighted VCI effects reach 1.1 percentage points, approximately 2.5 times the unweighted magnitude. The ordering of effects changes: in the weighted specification, ESI generates the largest long-run impact, followed by VCI and SMI.

The divergence between quantity and price responses for ESI is particularly revealing. While Section 4.1 demonstrated that ESI does not capture binding physical constraints on export availability, the CPI results show that early-stage water stress signals nonetheless affect prices through market expectations. Panel (a) of Figure 5 shows that even unweighted ESI generates delayed but persistent CPI increases, and Panel (a) of Figure 6 demonstrates that this effect is dramatically magnified when major exporters are weighted by their market shares. This pattern is consistent with agricultural futures markets incorporating drought information rapidly into prices, even when the ultimate harvest impact remains uncertain. When evapotranspiration anomalies emerge in the U.S. Corn Belt or Brazil’s Mato Grosso, futures markets react immediately, generating precautionary price increases that transmit to Korean CPI despite limited effects on actual import volumes. The weighted specification magnifies this effect, confirming that ESI anomalies in major exporting regions command a mar-

ket risk premium that is absent in aggregate unweighted measures.

The amplification under import-share weighting underscores Korea’s structural vulnerability to drought shocks in a small number of dominant suppliers. The United States and Brazil collectively account for the majority of Korean grain and oilseed imports, and drought conditions in these regions generate disproportionate price effects relative to their contribution to global production. The weighted results demonstrate that this concentration risk operates through both physical availability constraints (VCI and SMI) and market expectation channels (ESI). A one-standard-deviation deterioration in weighted VCI or ESI translates into domestic grain inflation of 1.0–1.3 percentage points over the subsequent 12–18 months, even after controlling for global commodity prices and domestic macroeconomic conditions. These magnitudes are economically substantial and highlight the inflation forecasting value of satellite-based drought monitoring for a structurally import-dependent economy.

V. CONCLUSION

This paper quantifies the dynamic transmission of climate shocks from major agricultural exporting regions into Korean food and feed imports using satellite-derived drought indicators as proxies for physical supply constraints. Combining monthly trade data with vegetation, evapotranspiration, and soil moisture indices from MODIS and ERA5-Land, I estimate impulse responses via panel local projections that control for global commodity prices, exchange rates, and macroeconomic conditions. The estimated coefficients isolate supply-side disruptions net of information already reflected in market prices, enabling direct measurement of how biophysical constraints propagate into trade flows and domestic inflation.

The analysis yields three main findings. First, vegetation and soil moisture indices capture economically significant physical supply shocks: a one-standard-deviation increase in drought severity (sign-inverted VCI or SMI) generates cumulative import reductions of 13–17 percentage points, with peak contractionary effects occurring three to eight months after the shock. ESI exhibits negligible effects on import quantities, suggesting that evapotranspiration anomalies do not constitute binding constraints on export availability once vegetation and soil conditions are accounted for.

Second, VCI emerges as the most powerful and immediate proxy for supply disruptions. Import quantities contract by 8 percentage points within two months of a vegetation-based drought shock and reach peak declines of 15 percentage points by month five. This faster trans-

mission relative to soil moisture shocks reflects the direct linkage between satellite-observed vegetation stress and harvestable biomass: when NDVI indicates severe wilting during critical reproductive stages, the physical constraint on exportable supply materializes rapidly. In contrast, SMI exhibits a delayed buildup, with effects emerging only after three months and peaking around months five through six, consistent with the biological lag between root-zone moisture deficits at planting and subsequent yield losses. Crucially, these effects remain large and statistically significant even after controlling for contemporaneous global commodity prices, confirming that satellite indices capture supply disruptions orthogonal to price-mediated market adjustments.

Third, the transmission extends beyond import quantities into domestic food inflation. Korea's grain CPI increases by 0.3–0.7 percentage points in response to unweighted drought shocks, with VCI and SMI generating the largest effects consistent with their role as physical supply constraint proxies. The response to ESI, while negligible for quantities, is positive and statistically significant for prices, revealing that early-stage evapotranspiration anomalies operate through market expectation channels rather than binding physical constraints. When drought indices are weighted by each exporter's share in Korea's import basket, effects amplify dramatically: weighted VCI and ESI shocks generate domestic grain inflation of 1.0–1.3 percentage points over 12–18 months. This amplification reflects Korea's concentration risk—the United States and Brazil collectively account for the majority of grain and oilseed imports, and drought conditions in these dominant suppliers generate disproportionate price impacts through both physical availability constraints and market risk premia.

Disaggregation by origin and commodity reveals substantial heterogeneity (Appendix B). Brazilian imports exhibit particularly large drought sensitivity (20–30 percentage point declines), consistent with Brazil's dominant role in global soybean markets and the concentration of production in Mato Grosso. Russian and Canadian imports show similarly large elasticities, with timing patterns reflecting hemisphere-specific harvest calendars. Across commodities, cereals (HS 10) exhibit the largest responses (20–30 percentage points), reflecting their centrality to food security and limited substitutability, while oilseeds (HS 12) show more moderate effects (10–20 percentage points), likely due to greater storage capacity and industrial flexibility.

From a policy perspective, these findings demonstrate that real-time satellite monitoring provides actionable early warnings for strategic reserve management, supplier diversification, and inflation forecasting. For an economy where consumer food prices stand 45–50 percent above the OECD average and grain self-sufficiency hovers near 20 percent, a one-standard-deviation drought shock in

major exporting regions implies 10–30 percentage point reductions in import quantities and up to 1.3 percentage points of domestic grain inflation over the subsequent year. The fast transmission of VCI shocks—with significant effects within two to three months—enables near-term reserve decisions and forward contracting. The operational availability of MODIS NDVI at 16-day intervals and VCI's transparency suggest that drought early-warning systems should prioritize vegetation condition indices for trade and inflation forecasting applications.

Crucially, the predictive power of satellite indices remains robust even after controlling for global commodity prices. This orthogonality validates the independent value of satellite monitoring beyond merely tracking market prices: vegetation and soil moisture signals capture physical availability risks—such as logistical bottlenecks, quality degradation, or contract force majeure—that are not fully priced in contemporaneous spot markets. This information advantage is particularly valuable for import-dependent economies with limited supplier diversification options.

Limitations.

Two limitations suggest directions for future research. First, the regional drought indicators are constructed using rectangular bounding boxes that approximate core production zones rather than exact agro-ecological boundaries. While this choice ensures computational tractability and consistent Earth Engine extraction, it inevitably introduces measurement error relative to more detailed geo-referenced production maps. Future work should validate the robustness of the estimated impulse responses to alternative geospatial definitions, such as administrative-region masks, crop-suitability grids, or production-weighted averaging schemes that place greater weight on high-yield areas within each exporting country.

Second, the current framework does not separately identify import demand and export supply responses to climate shocks. The estimated local projections capture the joint adjustment of Korean importers and foreign producers to publicly available drought information, but they cannot disentangle changes in Korean demand (e.g., precautionary buying or stockpiling) from shifts in exporter supply driven by expected harvest outcomes. Extending the framework to incorporate exporter-side production and harvest statistics, as well as domestic Korean utilization and feed-demand indicators, would allow a more structural decomposition of the observed trade elasticities into supply and demand components. Such decomposition would clarify whether the import reductions documented here primarily reflect export rationing by suppliers or demand destruction by Korean importers facing

higher prices.

Notwithstanding these limitations, the evidence presented here demonstrates that satellite-based drought monitoring offers a practical tool for tracking food security risks as agricultural production concentrates in a small number of exporting regions.

Appendix A: Price Response Analysis

This appendix presents the impulse response functions for import unit values (dollars per kg), which serve as proxies for import prices. Figure 7 displays the response of aggregate grain import unit values to one-standard-deviation shocks in the Vegetation Condition Index (VCI), Evaporative Stress Index (ESI), and Soil Moisture Index (SMI).

As noted in the main text regarding import quantities, the dynamic adjustment of prices closely mirrors the quantity results. The responses to VCI and SMI shocks are positive and statistically significant, indicating that favorable climate conditions (supply expansion) tend to stabilize or slightly improve unit values in the aggregate, likely reflecting a volume effect that dominates pure price substitution in the short run. Conversely, the response to ESI remains statistically insignificant, consistent with its limited predictive power for import quantities.

These results underscore the structural vulnerability of the Korean food system. In the face of adverse climate shocks, both import volumes and value terms tend to deteriorate simultaneously. The similarity between quantity and price dynamics confirms that the "quantity" results presented in the baseline analysis are robust and reflective of the broader economic adjustment to climate signals.

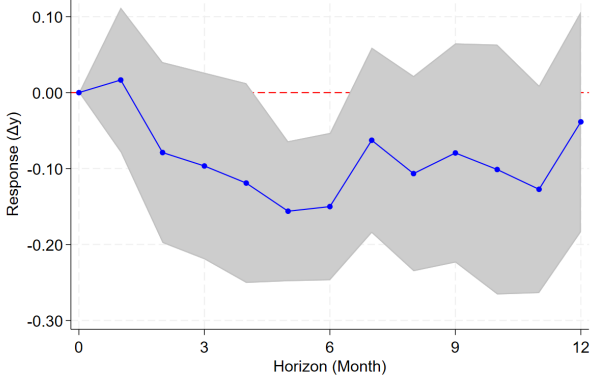
Appendix A: Country- and Commodity-Specific Impulse Responses

This appendix reports disaggregated impulse responses along specific origin-country and commodity pathways, complementing the aggregate analysis in Section 4.1. All drought indices are sign-inverted as described in Section 2.2, so that positive shocks represent increased drought severity. Consequently, negative estimated coefficients indicate that drought conditions reduce import flows, as expected under binding supply constraints.

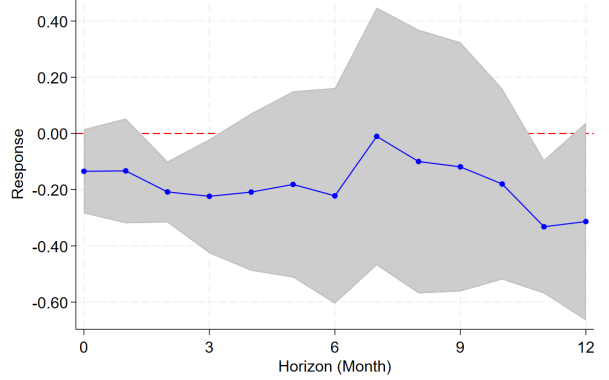
1. Country-Specific Transmission

Figure 8 presents impulse responses for selected country-specific pathways, revealing substantial heterogeneity in the transmission of drought shocks across origins.

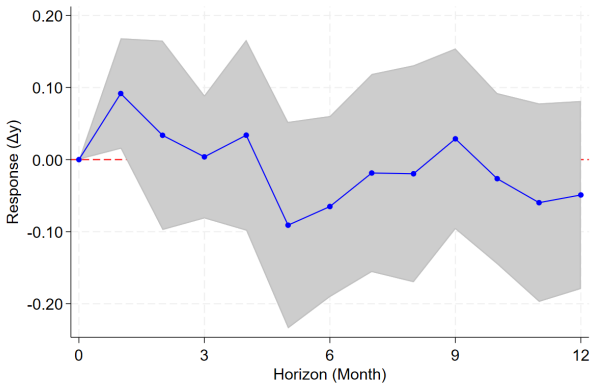
Panel (a) reports the response of imports from Brazil to a VCI shock in the Mato Grosso region, the center of Brazilian soybean and maize production. The response is negative and persistent, declining from zero at



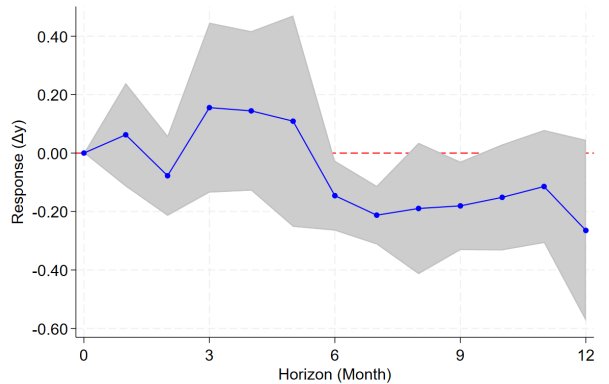
(a) Response to VCI Shock



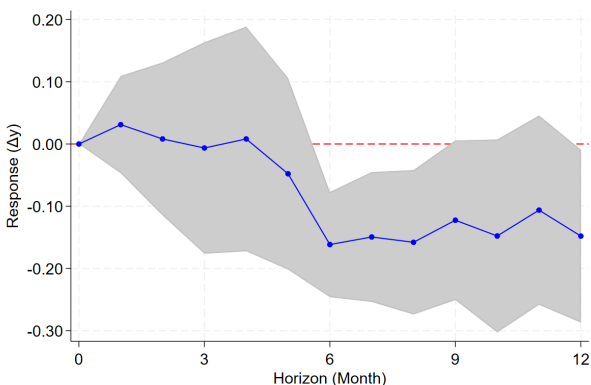
(a) Brazil: VCI Shock



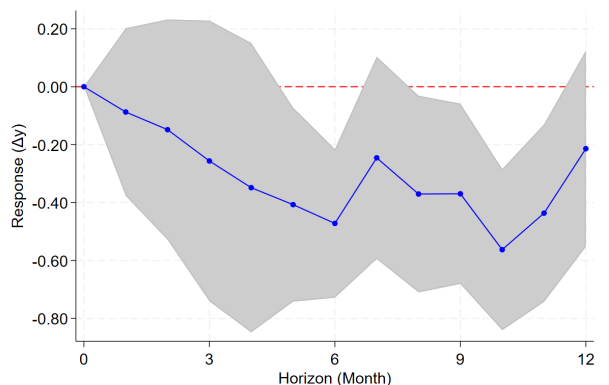
(b) Response to ESI Shock



(b) Brazil: SMI Shock



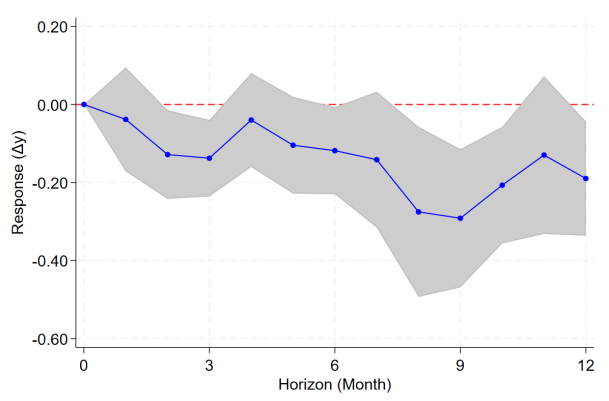
(c) Response to SMI Shock



(c) Russia: VCI Shock

FIG. 7: Impulse Response of Import Unit Values to Drought Index Shocks

impact to approximately -20 to -30 percentage points by month eight, with wide confidence intervals reflecting the smaller sample size for the Brazil-only subsample. This large elasticity is consistent with Brazil's role as the world's leading soybean exporter and a major supplier to Korea. Drought conditions in Mato Grosso during the growing season constrain harvestable area and yields,



(d) Canada: SMI Shock

FIG. 8: Country-Specific Impulse Responses to Drought Shocks

generating substantial reductions in export availability that Korean importers cannot easily offset through supplier diversification. The relatively late trough around month eight reflects the timing of the Brazilian soybean harvest, which occurs in the first quarter of the calendar year, with shipments reaching Korean ports approximately two to three months after harvest.

Panel (b) shows a similar pattern for soil moisture shocks in Brazil, with the response declining to approximately -25 to -30 percentage points around months seven through nine. The timing aligns with the critical planting and early growth period for Brazilian summer crops, during which soil moisture availability determines final planted area and sets the stage for subsequent yield outcomes. The large magnitude and persistence underscore the importance of Brazilian supply conditions for Korean food security: disruptions in South American production are difficult to offset given the scale and specialization of Brazilian agribusiness.

Panel (c) reports the response to VCI shocks in Russia. The effect is negative throughout the year, declining from approximately -15 to -20 percentage points in the first months to -25 to -30 percentage points by month twelve, with some volatility in the middle months. Russian wheat exports to Korea are subject to greater seasonal and policy-driven variation than those from other major suppliers, and the estimated response may partly reflect the interaction of climate shocks with domestic grain reserve policies and export restrictions that respond to domestic harvest outcomes. Nonetheless, the negative and sustained effect confirms that drought conditions in Russia's Southern agricultural regions translate into reduced export availability and lower Korean import volumes.

Panel (d) reports the response to soil moisture shocks in the Canadian Prairies, the primary source of Canadian wheat, canola, and pulses exported to Korea. The response is negative and sustained, declining to approximately -25 to -30 percentage points by month six and remaining near that level through the end of the year. Canada's spring wheat and canola crops are particularly sensitive to soil moisture at planting: limited precipitation during the short growing season leaves little margin for early-season water deficits. The large and persistent response to SMI shocks reflects this agronomic reality and highlights the value of soil moisture monitoring as an early indicator of Canadian export disruptions.

2. Commodity-Specific Transmission

Figure 9 disaggregates responses by HS chapter, revealing differential drought sensitivity across commodity categories.

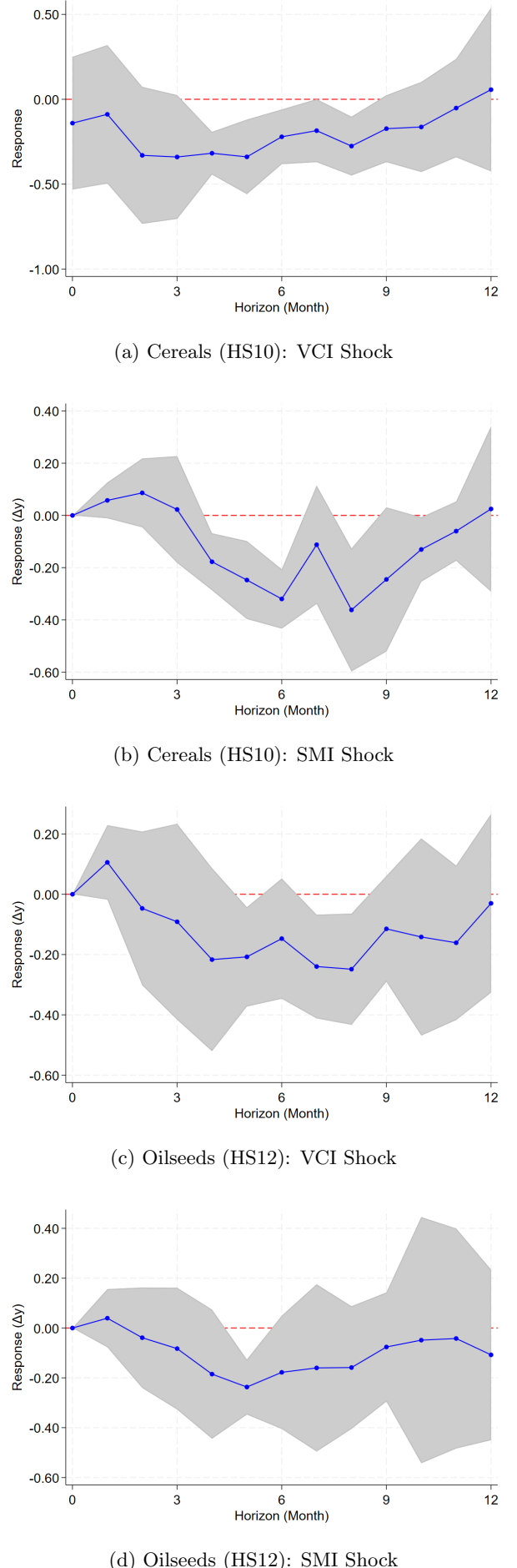


FIG. 9: Commodity-Specific Impulse Responses

Panels (a) and (b) report responses for HS chapter 10, which includes wheat, maize, rice, and barley. For VCI shocks, the response is strongly negative and sustained, declining to -20 to -25 percentage points by months three through eight. For SMI shocks, the response peaks near -25 percentage points around month four and remains elevated through the end of the year. These large elasticities reflect the fact that cereals are the core of Korea's food security concerns and exhibit relatively low domestic production, making imports highly sensitive to global supply conditions. A one-standard-deviation deterioration in vegetation or soil moisture conditions in major wheat and maize exporting regions reduces Korean cereal imports by roughly one-quarter over the subsequent year, even after controlling for exchange rates, energy prices, and global risk factors.

Panels (c) and (d) present the corresponding results for HS chapter 12, which covers oilseeds including soybeans, rapeseed, and sunflower seeds. The response patterns are qualitatively similar to those for cereals, with negative and delayed adjustments peaking in the three- to six-month window. However, the magnitudes are somewhat smaller, with VCI shocks generating peak responses around -10 to -15 percentage points and SMI shocks generating responses in the -10 to -20 percentage point range. This difference may reflect the greater substitutability and storage capacity in oilseed markets relative to food grains, allowing importers to smooth supply shocks over a longer horizon. Additionally, soybeans and other oilseeds are used primarily as feedstock for livestock and industrial processing rather than direct human consumption, reducing the urgency of precautionary imports in response to drought signals.

-
- [1] T. Iizumi, N. Ramankutty, S. Park, G. Sakurai, and M. Okada, Impacts of el niño southern oscillation on the global yields of major crops, *Nature Communications* **5**, 3712 (2014).
 - [2] R. M. Adams, C. Chen, B. A. McCarl, and et al., The economic effects of climate change on us agriculture, *Agricultural and Resource Economics Review* **28**, 96 (1999).
 - [3] W. Schlenker and M. J. Roberts, Nonlinear temperature effects indicate severe damages to us crop yields under climate change, *Proceedings of the National Academy of Sciences* **106**, 15594 (2009).
 - [4] O. Deschênes and M. Greenstone, The economic impacts of climate change: evidence from agricultural output and random fluctuations in weather, *American Economic Review* **97**, 354 (2007).
 - [5] F. Liu, The impact of climate disaster on international trade, *International Journal of Disaster Risk Reduction* **97**, 10.1016/j.ijdrr.2023.103218 (2023).
 - [6] F. Amodio, L. Baccini, G. Chiovelli, and M. Di Maio, Weather shocks affect trade policy: Evidence from preferential trade agreements, *American Journal of Agricultural Economics* **107**, 696 (2025).
 - [7] J. Baffes, M. A. Kose, F. Ohnsorge, and M. Stocker, The transmission of food and energy prices: Searching for the missing link, *Journal of Commodity Markets* **1**, 1 (2015).
 - [8] N. Minot, Transmission of world food price changes to markets in sub-saharan africa, *International Food Policy Research Institute Discussion Paper* **1059** (2011).
 - [9] M. E. Brown, B. Hintermann, and N. Higgins, Markets, climate change, and food security in west africa, *Environmental Science & Technology* **43**, 8016 (2009).
 - [10] G. V. Lehecka, X. Wang, and P. Garcia, The value of usda crop progress and condition information: reactions of corn and soybean futures to usda reports, *Applied Economic Perspectives and Policy* **37**, 612 (2015).
 - [11] M. J. Roberts and W. Schlenker, Weather and the long-run dynamics of grain prices, *Marketing and Agricultural Economics* **84**, 135 (2013).
 - [12] F. N. Kogan, Application of vegetation index and brightness temperature for drought detection, *Advances in Space Research* **15**, 91 (1995).
 - [13] F. N. Kogan, Global drought watch from space, *Bulletin of the American Meteorological Society* **78**, 621 (1997).
 - [14] M. C. Anderson, C. Hain, B. Wardlow, A. Pimstein, J. R. Mecikalski, and W. P. Kustas, Evaluation of drought indices based on thermal remote sensing of evapotranspiration over the continental united states, *Journal of Climate* **24**, 2025 (2011).
 - [15] J. Muñoz-Sabater, E. Dutra, A. Agustí-Panareda, C. Albergel, G. Arduini, G. Balsamo, S. Bousetta, M. Choulga, S. Harrigan, H. Hersbach, et al., ERA5-Land: a state-of-the-art global reanalysis dataset for land applications, *Earth System Science Data* **13**, 4349 (2021).
 - [16] C. Funk, L. Harrison, S. Shukla, et al., Recognizing the famine early warning systems network: over 30 years of drought early warning science advances and partnerships promoting global food security, *Bulletin of the American Meteorological Society* **100**, 1011 (2019).
 - [17] M. E. Brown and C. C. Funk, Food security under climate change, *Science* **319**, 580 (2008).
 - [18] D. M. Johnson, Crop yield forecasting on the canadian prairies by remotely sensed vegetation indices and machine learning methods, *Agricultural and Forest Meteorology* **218**, 74 (2014).
 - [19] J. A. Otkin, M. Svoboda, E. D. Hunt, et al., Flash droughts: A review and assessment of the challenges imposed by rapid-onset droughts in the united states, *Bulletin of the American Meteorological Society* **99**, 911 (2018).
 - [20] Ò. Jordà, Estimation and inference of impulse responses by local projections, *American Economic Review* **95**, 161 (2005).
 - [21] M. Plagborg-Møller and C. K. Wolf, Local projections and vars estimate the same impulse responses, *Econometrica* **89**, 955 (2021).
 - [22] Regional bounding boxes are defined as follows (longitude-latitude coordinates): U.S. Corn Belt [96°W–89°W, 40°N–43°N], Brazil's Mato Grosso [58°W–52°W, 15°S–11°S], Australia's Wheat Belt [116°E–119°E, 34°S–31°S], Canada's Prairies [109°W–104°W, 50°N–53°N], and Russia's South [38°E–42°E, 45°N–48°N]. Argentina's Pampas [64°W–60°W, 35°S–32°S] and Ukraine's Cher-

nozem [30°E–35°E, 48°N–50°N] are constructed but excluded from baseline estimation due to incomplete control variable coverage. The regional bounding boxes are chosen to capture the core production zones within each country, rather than full administrative or agronomic definitions of each region. For example, the U.S. Corn Belt rectangle centers on Iowa and its surrounding high-yield counties, which consistently account for the highest shares of U.S. corn and soybean output. Using compact rectangular regions ensures consistent Earth Engine extraction, minimizes missing-pixel artifacts near irregular administrative borders, and focuses the drought indicators on the areas where climatic stress is most likely to

translate into global price and trade fluctuations. This rectangular definition is, however, an approximation to the true agro-ecological production zones, and future work will validate the robustness of the results to alternative geospatial definitions such as administrative-region masks or crop-specific suitability maps.

- [23] S. R. Baker, N. Bloom, and S. J. Davis, Measuring economic policy uncertainty, *The Quarterly Journal of Economics* **131**, 1593 (2016).
- [24] D. Caldara and M. Iacoviello, Measuring geopolitical risk, *American Economic Review* **112**, 1194 (2022).
- [25] R. E. Whaley, The investor fear gauge, *Journal of Portfolio Management* **26**, 12 (2000).